Toward Designed Assembly of Microporous Coordination Networks Constructed from Silver(I)−Hexamethylenetetramine Layers

Shao-Liang Zheng,[†] Ming-Liang Tong,*[,†] Ruo-Wen Fu,[†] Xiao-Ming Chen,*[,†] and Seik-Weng Ng[‡]

School of Chemistry & Chemical Engineering, Zhongshan University, Guangzhou 510275, China, and Institute of Postgraduate Studies and Research University of Malaya, 50603 Kuala Lumpur, Malaysia

Received November 8, 2000

Eight interesting microporous networks based on 2-D [Ag(μ_3-hmt)] (hmt = hexamethylenetetramine) layers were obtained via rational synthetic strategies. Out of these products isolated and structurally characterized, six present a metal-to-hmt molar ratio of 1:1 and contain 2-D coordination layers assembled by 2-D Ag(I)-hmt networks with aromatic monocarboxylates, which are [Ag(μ_3-hmt)(*p*-nba)]·2.5H_2O (**1**), [Ag(μ_3-hmt)(*m*-nba)]·2.5H_2O (**2**), [Ag(μ_3-hmt)(dnba)] (**3**), [Ag(μ_3-hmt)(α-hna)](EtOH) (**4**), [Ag(μ_3-hmt)(β-hna)](EtOH) (**5**), and [Ag(μ_3-hmt)(noa)]-(H_2O)(EtOH) (**6**) (*p*-nba = 4-nitrobenzoate, *m*-nba = 3-nitrobenzoate, dnba = 3,5-dinitrobenzoate, α-hna = 1-hydroxy-2-naphthate, β-hna = 3-hydroxy-2-naphthate, and noa = 2-naphthoxyacetate), and two present a metal-to-hmt molar ratio of 2:1 and contain 3-D microporous networks constructed from the 2-D Ag-hmt layers and linear dicarboxylates as molecular pillars, which are [Ag_2(μ_3-hmt)$_2$(fa)]·4H_2O (**7**) and [Ag_2(μ_3-hmt)$_2$(adp)]·8H_2O (**8**) (fa = fumarate and adp = adipate). The result shows that the pore sizes may be tuned with different carboxylates. Gas adsorption measurements were performed to confirm the microporosity of these coordination open frameworks.

Introduction

The chemistry of microporous compounds has been studied extensively because of their intriguing applications including selective separation, gas adsorption, and heterogeneous catalysis. Recently construction of microporous networks by copolymerization of organic molecules with metal ions has received intensive attention,[1] since these structures have the potential for more flexible rational design and tailoring. A number of such coordination polymer architectures have been synthesized,[2,3] demonstrating that the hope of rational synthesis is running high, though it is still challenging. Usually, the network topology can be designed by selecting the coordination geometry of metal ions and the chemical structure of organic ligands. We and others have found that hexamethylenetetramine (hmt) can act as a polydentate ligand for self-assembly of topologically interesting Ag-hmt architectures in the presence of small anions.[4−10] Some of these networks are stable, two-dimensional (2-D) wavy coordination layers,[6c,8b] in which the Ag(I) atoms are commonly in T-shaped or tetrahedral geometry and one of the coordinate sites is usually occupied by a small and labile ligand (such as NO_3^-, NO_2^-, $S_2O_6^{2-}$, or ClO_4^-). A careful examination of the detailed geometric data reveals that the labile ligands (and the metal atoms) are arranged in rows with regular

* Corresponding author. E-mail: cescxm@zsu.edu.cn (X.-M.C.).
[†] Zhongshan University.
[‡] Institute of Postgraduate Studies and Research University of Malaya.

(1) (a) Janiak, C. *Angew. Chem., Int. Ed. Engl.* **1997**, *36*, 1431. (b) Batten, S. R.; Robson, R. *Angew. Chem., Int. Ed.* **1998**, *37*, 1460. (c) Yaghi, O. M.; Li, H.; Davis, C.; Richardson, D.; Groy, T. L. *Acc. Chem. Res.* **1998**, *31*, 474. (d) Munakata, M.; Wu, L.; Kuroda-Sowa, T. *Adv. Inorg. Chem.* **1999**, *46*, 173. (e) Kitagawa, S.; Kondo, M. *Bull. Chem. Soc. Jpn.* **1998**, *71*, 1735. (f) Blake, A. J.; Champness, N. R.; Hubberstey, P.; Li, W.-S.; Withersby, M. A.; Schröder, M. *Coord. Chem. Rev.* **1999**, *183*, 117. (g) Hagrman, P. J.; Hagrman, D.; Zubieta, J. *Angew. Chem., Int. Ed.* **1999**, *38*, 2639.

(2) (a) Tong, M.-L.; Yu, X.-L.; Chen, X.-M.; Mak, T. C. W. *J. Chem. Soc., Dalton Trans.* **1998**, 5. (b) Tong, M.-L.; Ye, B.-H.; Cai, J.-W.; Chen, X.-M.; Ng, S. W. *Inorg. Chem.* **1998**, *37*, 2645. (c) Tong, M.-L.; Cai, J.-W.; Yu, X.-L.; Chen, X.-M. S. W. Ng,; Mak, T. C. W. *Aust. J. Chem.* **1998**, *51*, 637. (d) Ye, B.-H.; Chen, X.-M.; Xue, G.-Q.; Ji, L.-N. *J. Chem. Soc., Dalton Trans.* **1998**, 2827. (e) Tong, M.-L.; Lee, H. K.; Chen, X.-M.; Huang, R.-B.; Mak, T. C. W. *J. Chem. Soc., Dalton Trans.* **1999**, 3657. (f) Tong, M.-L.; Chen, X.-M.; Ye, B.-H.; Ji, L.-N. *Angew. Chem., Int. Ed.* **1999**, *38*, 2237. (g) Yang, G.; Zheng, S.-L.; Chen, X.-M. *Inorg. Chim. Acta* **2000**, *233*, 86. (h) Tong, M.-L.; Chen, H.-J.; Chen, X.-M. *Inorg. Chem.* **2000**, *39*, 2235. (i) Yang, S.-P.; Chen, X.-M.; Ji, L.-N. *J. Chem. Soc., Dalton Trans.* **2000**, 2337. (j) Chen, H.-J.; Zhang, L.-Z.; Cai, Z.-G.; Yang, G.; Chen, X.-M. *J. Chem. Soc., Dalton Trans.* **2000**, 2463. (k) Tong, M.-L.; Chen, X.-M.; Ng, S. W. *Inorg. Chem. Commun.* **2000**, *3*, 436.

(3) (a) Eddaoudi, M.; Li, H.; Yaghi, O. M. *J. Am. Chem. Soc.* **2000**, *122*, 1391. (b) Kondo, M.; Yoshitomi, T.; Seki, K.; Matsuzaka, H.; Kitagawa, S. *Angew. Chem., Int. Ed. Engl.* **1997**, *37*, 11725. (c) Reineke, T. M.; Eddaoudi, M.; O'Keeffe, M.; Yaghi, O. M. *Angew. Chem., Int. Ed.* **1999**, *38*, 2590. (d) Li, H.; Eddaoudi, M.; O'Keeffe, M.; Yaghi, O. M. *Nature* **1999**, *402*, 276. (e) Noro, S.-I.; Kitagawa, S.; Kondo. M.; Seki, K. *Angew. Chem., Int. Ed.* **2000**, *39*, 2081. (f) Li, H.; Eddaoudi, M.; Groy, T. L.; Yaghi, O. M. *J. Am. Chem. Soc.* **1998**, *120*, 8571.

(4) (a) Carlucci, L.; Ciani, G.; Proserpio, D. M.; Sironi, A. *J. Am. Chem. Soc.* **1995**, *117*, 12861. (b) Carlucci, L.; Ciani, G.; Proserpio, D. M.; Sironi, A. *Inorg. Chem.* **1997**, *36*, 1736.

(5) Michelet, A.; Voissat, B.; Khodadad, P.; Rodier, N. *Acta Crystallogr., Sect. B* **1981**, *37*, 2171.

(6) (a) Carlucci, L.; Ciani, G.; Gudenberg, D. W. V.; Proserpio, D. M.; Sironi, A. *J. Chem. Soc., Chem. Commun.* **1997**, 631. (b) Bertelli, M.; Carlucci, L.; Ciani, G.; Proserpio, D. M.; Sironi, A. *J. Mater. Chem.* **1997**, *7*, 1271. (c) Carlucci, L.; Ciani, G.; Proserpio, D. M.; Rizzato, S. *J. Solid State Chem.* **2000**, *152*, 211.

(7) Batten, S. R.; Hoskins, B. F.; Robson, R. *Inorg. Chem.* **1998**, *37*, 3432.

(8) (a) Tong, M.-L.; Zheng, S.-L.; Chen, X.-M. *Chem. Commun.* **1999**, 561. (b) Tong, M.-L.; Zheng, S.-L.; Chen, X.-M. *Chem. Eur. J.* **2000**, *6*, 3729. (c) Zheng, S.-L.; Tong, M.-L.; Yu, X.-L.; Chen, X.-M. *J. Chem. Soc., Dalton Trans.* **2001**, 586.

(9) (a) Tong, M.-L.; Zheng, S.-L.; Chen, X.-M. *Procedings of 2nd China-Korea Joint Symposium on Inorganic Chemistry*, Nanjing, October 1998; pp 29−30. (b) Bu, W. M.; Ye, L.; Fan, Y. G. *Inorg. Chem. Commun.* **2000**, *3*, 194.

(10) (a) Mak, T. C. W. *Inorg. Chim. Acta* **1984**, *84*, 19. (b) Mak, T. C. W. *Jiegou Huaxue* (*Chin. J. Struct. Chem.*) **1985**, *4*, 16.

10.1021/ic001237z CCC: $20.00
Published on Web 06/05/2001

Chart 1. Two Possible Routes for Rational Organization of the 2-D Hexagonal Ag(I)-hmt Coordination Layers into 3-D Networks.

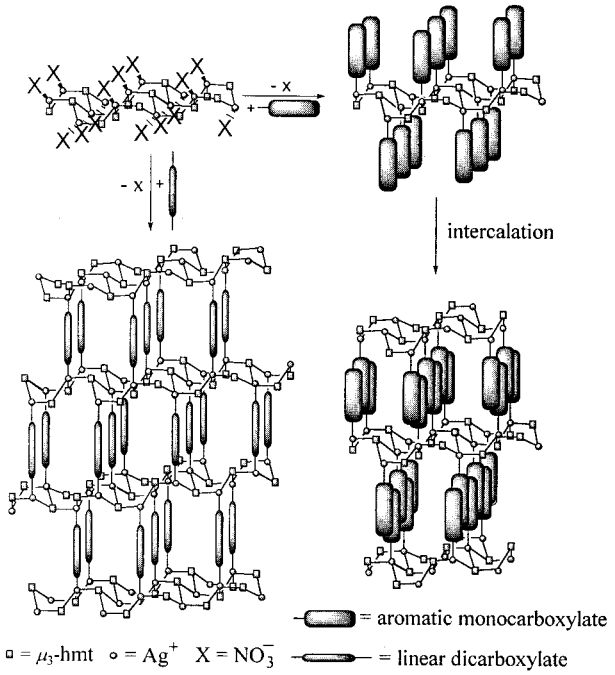

intra- and inter-row spacings of ca. 6.6 and 10.5 Å, respectively. The intra-row spacing is about twice the face-to-face distance between a pair of strongly stacked aromatic groups. This fact encouraged us to explore the possible routes for rational organization of the 2-D hexagonal Ag(I)-hmt coordination layers into some kind of 3-D network with porous structures (Chart 1, also see below). The first possible route is utilization of aromatic monocarboxylates, having the ability of $\pi-\pi$ stacking interaction, to replace the small and labile anions of the 2-D [Ag(μ_3-hmt)X] (X = small and labile anions) layer, and the resulting layers can be further extended into 3-D supramolecular arrays; the second one is utilization of the bridging dicarboxylate spacers (or molecular pillars) to replace the small and labile anions of the [Ag(μ_3-hmt)X] layer, and then pillar adjacent 2-D layers into stable 3-D coordination networks with channels.[9a] We report herein the systematic preparations and crystal structures of eight coordination open networks, namely, [Ag(μ_3-hmt)(*p*-nba)]·2.5H_2O (**1**), [Ag(μ_3-hmt)(*m*-nba)]·2.5H_2O (**2**), [Ag(μ_3-hmt)(dnba)] (**3**), [Ag(μ_3-hmt)(α-hna)](EtOH) (**4**), [Ag(μ_3-hmt)(β-hna)](EtOH) (**5**), [Ag(μ_3-hmt)(noa)](H_2O)(EtOH) (**6**), [Ag_2(μ_3-hmt)$_2$(fa)]·4H_2O (**7**), and [Ag_2(μ_3-hmt)$_2$(adp)]·8H_2O (**8**) (*p*-nba = 4-nitrobenzoate, *m*-nba = 3-nitrobenzoate, dnba = 3,5-dinitrobenzoate, α-hna = 1-hydroxy-2-naphthate, β-hna = 3-hydroxy-2-naphthate, noa = 2-naphthoxyacetate, fa = fumarate, and adp = adipate). Among them, **1**−**3** are new 2-D coordination layers assembled by Ag(I)-hmt complexes with benzoates as lateral ligands, which are intercalated into 3-D networks by strong interlayer $\pi-\pi$ stacking interaction between the aromatic groups. Complexes **4**−**6** have 2-D coordination layers similar to those of **1**−**3** and are further extended into different 3-D supramolecular arrays via C−H···π or weak $\pi-\pi$ stacking interaction without direct or significant intercalation of the lateral ligands (Chart 2, also see below), which are different from those of **1**−**3** and are somewhat out of our anticipation, while **7** and **8** are two microporous 3-D coordination networks constructed from 2-D [Ag(μ_3-hmt)] layers and linear dicarboxylates of different lengths as molecular pillars.

Chart 2. 3-D Supramolecular Arrays Based on the 2-D Hexagonal Coordination Layers and the C−H···π and Offset $\pi-\pi$ Stacking Interactions in **4**−**6**

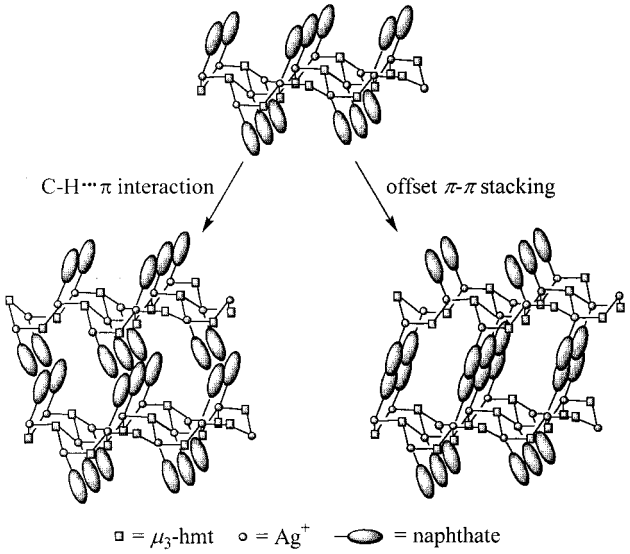

The gas adsorption measurements were performed to confirm the microporosity in these open coordination frameworks.

Experimental Section

Materials and Physical Measurements. Ag(μ_3-hmt)NO_3, Ag_2(fa), and Ag_2(adp) were prepared according to the literature methods.[5,11] Other reagents and solvents employed were commercially available and used as received without further purification. The C, H, N microanalyses were carried out with a Perkin-Elmer 240 elemental analyzer. The FT-IR spectra were recorded from KBr pellets in the range 4000−400 cm^{-1} on a Nicolet 5DX spectrometer. Thermogravimetric data were collected on a Perkin-Elmer TGS-2 analyzer in flowing dinitrogen at a heating rate of 10 °C/min. Gas adsorption measurements were carried out with a Micromeritics ASAP 2010 surface area and porosimetry system. The gas adsorption tests of the desolvate **1**, **6**, and **8** were obtained from the N_2 gas adsorption at 77 K with a volumetric adsorption apparatus. After **1** (292.8 mg), **6** (811.4 mg), and **8** (843.6 mg) were placed at 80 °C under vacuum for 36 h, the sample lost weights of 10.1% (2.5H_2O), 12.2% (1EtOH and 1H_2O), and 19.1% (8H_2O) for **1**, **6**, and **8**, respectively, in agreement with the TGA results.

Synthesis. [Ag(μ_3-hmt)(*p*-nba)]·2.5H_2O (1). An aqueous solution (5 cm^3) of *p*-nitrobenzolic acid (0.16 g, 1.0 mmol) was added dropwise to a stirred MeCN−H_2O [2:1 (v/v); 5 cm^3] solution of Ag(μ_3-hmt)NO_3 (0.32 g, 1.0 mmol) at 50 °C for 30 min. The solution was adjusted to pH ≈ 8.5 by addition of an aqueous NH_3 solution. The resulting pale yellow solution was allowed to stand in air at room temperature for 2 weeks, yielding yellow crystals in good yield (78%). Anal. Calcd for $C_{13}H_{21}AgN_5O_{6.5}$, **1**: C, 34.00; H, 4.61; N, 15.25. Found: C, 34.12; H, 4.55; N, 15.23. IR (KBr, cm^{-1}): 3431m, br, 3111w, 2948m, 2849w, 1619s, 1585vs, 1522s, 1460m, 1385s, 1348vs, 1238vs, 1005vs, 923w, 870w, 827s, 803s, 728s, 688m, 658w, 505m.

[Ag(μ_3-hmt)(*m*-nba)]·2.5H_2O (2). It was prepared as for **1**, yield ca. 75%. Anal. Calcd for $C_{13}H_{21}AgN_5O_{6.5}$, **2**: C, 34.00; H, 4.61; N, 15.25. Found: C, 34.18; H, 4.55; N, 15.33. IR (KBr, cm^{-1}): 3409m, br, 2952m, 2882w, 1595vs, 1560s, 1525s, 1461m, 1426w, 1377s, 1349vs, 1236vs, 1075m, 1005vs, 927w, 906w, 807m, 723s, 688m, 667m, 512m.

[Ag(μ_3-hmt)(dnba)] (3). It was prepared as for **1**, yield ca. 75%. Anal. Calcd for $C_{13}H_{15}AgN_6O_6$, **3**: C, 34.01; H, 3.29; N, 18.30. Found: C, 34.07 H, 3.52; N, 18.62. IR (KBr, cm^{-1}): 3444m, br, 3093w,

(11) Mak, T. C. W.; Yip, W.-H.; Kennard, C. H. L.; Smith, G.; O'Reilly, E. J. *Aust. J. Chem.* **1986**, *39*, 541

Table 1. Crystal Data and Structure Refinement for Compounds **1**−**8**

	[Ag(μ_3-hmt)(*p*-nba)]·2.5H_2O (**1**)	[Ag(μ_3-hmt)(*m*-nba)]·2.5H_2O (**2**)	[Ag(μ_3-hmt)(dnba)] (**3**)	[Ag(μ_3-hmt)(α-hna)](EtOH) (**4**)
chemical formula	$C_{13}H_{21}AgN_5O_{6.5}$	$C_{13}H_{21}AgN_5O_{6.5}$	$C_{13}H_{15}AgN_6O_6$	$C_{19}H_{25}AgN_4O_4$
a (Å)	6.604(2)	6.621(2)	23.026(7)	12.154(10)
b (Å)	24.078(10)	23.534(7)	6.5270(10)	15.125(16)
c (Å)	10.514(6)	10.414(3)	10.466(4)	11.030(7)
β (deg)	93.38	94.250(10)	90	90
V (Å^3)	1668.9(13)	1618.2(8)	1572.9(8)	2028(3)
Z	4	4	4	4
fw	459.22	459.22	459.18	481.30
space group	$P2_1/n$ (No. 14)	$P2_1/n$ (No. 14)	*Pnma* (No. 62)	$Pca2_1$ (No. 29)
T (°C)	22(1)	22(1)	22(1)	22(1)
λ (Å) (Mo Kα)	0.71073	0.71073	0.71073	0.71073
ρ_{calcd} (g cm^{-3})	1.828	1.885	1.939	1.577
μ (mm^{-1})	1.254	1.293	1.330	1.026
R_1 ($I > 2\sigma(I)$)[a]	0.0478	0.0376	0.0380	0.0414
wR_2 (all data)[a]	0.1263	0.0987	0.0848	0.1110

	[Ag(μ_3-hmt)(β-hna)](EtOH) (**5**)	[Ag(μ_3-hmt)(noa)]-(H_2O)(EtOH) (**6**)	[Ag_2(μ_3-hmt)$_2$(fa)]·4H_2O (**7**)	[Ag_2(μ_3-hmt)$_2$-(adp)]·8H_2O (**8**)
chemical formula	$C_{19}H_{25}AgN_4O_4$	$C_{20}H_{29}AgN_4O_5$	$C_{16}H_{34}Ag_2N0_8$	$C_{18}H_{48}Ag_2N_8O_{12}$
a (Å)	12.256(8)	12.193(7)	17.228(8)	10.092(5)
b (Å)	15.028(8)	11.044(3)	11.979(4)	21.818(8)
c (Å)	11.013(3)	33.570(17)	11.177(5)	6.523(4)
V (Å^3)	2028.4(18)	4521(4)	2306.6(17)	1436.3(12)
Z	4	8	4	2
fw	481.30	513.34	682.25	784.38
space group	$Pca2_1$ (No. 29)	*Pbca* (No. 61)	*Pbcn* (No. 60)	*Pnnm* (No. 58)
T (°C)	22(1)	22(1)	22(1)	22(1)
λ (Å) (Mo Kα)	0.71073	0.71073	0.71073	0.71073
ρ_{calc} (g cm^{-3})	1.576	1.509	1.965	1.814
μ (mm^{-1})	1.026	0.929	1.759	1.435
R_1 ($I \geq 2\sigma(I)$)[a]	0.0461	0.0579	0.0499	0.0446
wR_2 (all data)[a]	0.1156	0.1490	0.1362	0.1264

[a] $R_1 = \sum||F_o| - |F_c||/\sum|F_o|$, $wR_2 = [\sum w(F_o^2 - F_c^2)^2/\sum w(F_o 2)^2]^{1/2}$, $w = [\sigma^2(F_o)^2 + (0.1(\max(0,F_o^2) + 2F_c^2)/3)^2]^{-1}$.

2952m, 2882w, 1623vs, 1581m, 1532vs, 1454m, 1342vs, 1236s, 1222m, 1075m, 1004vs, 990s, 920m, 828w, 800s, 723s, 688s, 660w, 519m.

[Ag(μ_3-hmt)(α-hna)](EtOH) (**4**). An aqueous solution (5 cm^3) of 1-hydroxy-2-naphthoic acid (0.19 g, 1.0 mmol) was added dropwise to a stirred CH_2Cl_2−MeOH−H_2O [10:10:1 (v/v); 5 cm^3] solution of Ag(μ_3-hmt)NO_3 (0.32 g, 1.0 mmol) at 50 °C for 30 min. The solution was adjusted to pH ≈ 8.5 by addition of an aqueous NH_3 solution. The resulting pale yellow solution was allowed to stand in air at room temperature for 2 weeks, yielding yellow crystals in good yield (70%). Anal. Calcd for $C_{19}H_{25}AgN_4O_4$, **4**: C, 47.41; H, 5.24; N, 11.64. Found: C, 47.42; H, 5.54; N, 11.52. IR (KBr, cm^{-1}): 3393s, 3382s, br, 3126m, 2990m, 2886m, 1621s, 1580vs, 1503vs, 1465m, 1402s, 1369m, 1309m, 1232vs, 1006vs, 925w, 871w, 807s, 777m, 724w, 688m, 657w, 601w, 575m, 533w, 447w.

[Ag(μ_3-hmt)(β-hna)](EtOH) (5). It was prepared as for **4** (yield ca. 78%). Anal. Calcd for $C_{19}H_{25}AgN_4O_4$, **5**: C, 47.41; H, 5.24; N, 11.64. Found: C, 47.32; H, 5.51; N, 11.58. IR (KBr, cm^{-1}): 3393s, 3375s, br, 3226m, 2950m, 2886m, 1648s, 1577vs, 1519vs, 1459s, 1407m, 1371m, 1341s, 1236vs, 1006vs, 919w, 873w, 845m, 804s, 782m, 749m, 692m, 664w, 623w, 592m, 515w, 476w.

[Ag(μ_3-hmt)(noa)](H_2O)(EtOH) (6). It was prepared as for **4** (yield ca. 82%). Anal. Calcd for $C_{20}H_{29}AgN_4O_5$ **6**: C, 47.79; H, 5.69; N, 10.91. Found: C, 47.72; H, 5.52; N, 10.82. IR (KBr, cm^{-1}): 3419m, br, 3056w, 2962m, 2891m, 1604vs, 1511m, 1466s, 1396m, 1329m, 1238vs, 1216s, 1179s, 1121w, 1053m, 1006vs, 836m, 809s, 745m, 693s, 667m, 626w, 512w, 474m.

[Ag_2(μ_3-hmt)$_2$(fa)]·4H_2O (7). An aqueous solution (5 cm^3) of hmt (0.140 g, 1.0 mmol) was added dropwise to a stirred MeCN−H_2O [2:1 (v/v); 5 cm^3] solution of Ag_2(fa) (0.336 g, 2.0 mmol) at 50 °C for 15 min. The resulting colorless solution was allowed to stand in air at room temperature for 2 weeks, yielding colorless crystals in good yield (82%). Anal. Calcd for $C_{16}H_{34}Ag_2N_8O_8$, **7**: C, 28.17; H, 5.02; N, 16.42. Found: C, 28.56; H, 4.95; N, 16.64. IR (KBr, cm^{-1}): 3393m, br, 2952m, 2873m, 1586vs, 1466m, 1395s, 1237vs, 1006vs, 812s, 672s, 570w, 513m.

[Ag_2(μ_3-hmt)$_2$(adp)]·4H_2O (8). It was prepared as for **7** (yield ca. 72%). Anal. Calcd for $C_{18}H_{48}Ag_2N_8O_{12}$, **7**: C, 27.56; H, 6.17; N, 14.29. Found: C, 27.68; H, 6.21; N, 14.42. IR (KBr, cm^{-1}): 3461m, br, 2930s, 2872s, 1567vs, 1456s 1404s, 1382s, 1328m, 1202m, 1129w, 1006vs, 912m, 818s, 729w, 689m, 673s, 586w, 511m.

X-ray Crystallography. Diffraction intensities for the eight complexes were collected at 21 °C on a Siemens R3m diffractometer using the ω-scan technique. Lorentz−polarization and absorption corrections were applied.[12] The structures were solved with direct methods and refined with full-matrix least-squares technique using the SHELXS-97 and SHELXL-97 programs, respectively.[13,14] Anisotropic thermal parameters were assigned to all non-hydrogen atoms. The organic hydrogen atoms were generated geometrically (C−H = 0.96 Å); the aqua hydrogen atoms were located from difference maps and refined with isotropic temperature factors. Analytical expressions of neutral-atom scattering factors were employed, and anomalous dispersion corrections were incorporated.[15] The absolute structures for **4** and **5** have been determined with the Flack parameters of 0.12(8) and 0.01(8), respectively.[16] In **8**, the adipate group is disordered and its atoms were refined with 1/4 site occupancies each with geometric restraints. The crystallographic data for **1**−**8** are listed in Table 1. The selected interatomic distances and angles for **1**−**8** are given in Table 2. Drawings were produced with SHELXTL.[17]

(12) North, A. C. T.; Phillips, D. C.; Mathews, F. S. *Acta Crystallogr., Sect. A* **1968**, *24*, 351.
(13) Sheldrick, G. M. *SHELXS-97, Program for Crystal Structure Solution*; Göttingen University, Germany, 1997.
(14) Sheldrick, G. M. *SHELXL-97, Program for Crystal Structure Refinement*; Göttingen University, Germany, 1997.
(15) *International Tables for X-ray Crystallography*; Kluwer Academic Publisher: Dordrecht, 1992; Vol. C, Tables 4.2.6.8 and 6.1.1.4.
(16) Flack, H. D. *Acta Crystallogr., Sect. A* **1983**, *39*, 876.

Table 2. Selected Interatomic Distances (Å) and Bond Angles (deg)

Complex **1**[a]			
Ag(1)−O(1)	2.367(4)	Ag(1)−N(2a)	2.378(3)
Ag(1)−N(4b)	2.426(4)	Ag(1)−N(1)	2.478(4)
O(1)···O(2w)	2.838(8)	O(2w)···O(3c)	3.028(8)
O(1w)···O(3w)	2.47(2)	O(3w)···O(3wd)	2.88(2)
O(1w)···O(2w)	2.51(2)	O(3w)···N(3e)	2.943(7)
O(1)−Ag(1)−N(2a)	130.2(1)	O(1)−Ag(1)−N(4b)	87.3(1)
N(2a)−Ag(1)−N(4b)	109.8(1)	O(1)−Ag(1)−N(1)	89.9(1)
N(2a)−Ag(1)−N(1)	117.0(1)	N(4b)−Ag(1)−N(1)	119.8(1)
Complex **2**[b]			
Ag(1)−N(1)	2.400(4)	Ag(1)−N(3a)	2.442(3)
Ag(1)−O(1)	2.403(4)	Ag(1)−N(4b)	2.484(4)
O(1)···O(1w)	2.803(6)	O(2w)···O(4c)	2.96(2)
O(2w)···O(3w)	2.63(4)	O(3w)···N(2d)	2.896(12)
N(1)−Ag(1)−O(1)	136.6(1)	N(1)−Ag(1)−N(3a)	103.3(1)
O(1)−Ag(1)−N(3a)	92.4(1)	N(1)−Ag(1)−N(4b)	116.6(1)
O(1)−Ag(1)−N(4b)	90.2(1)	N(3a)−Ag(1)−N(4b)	116.7(1)
Complex **3**[c]			
Ag(1)−O(1)	2.322(5)	Ag(1)−N(3b)	2.394(3)
Ag(1)−N(3a)	2.394(3)	Ag(1)−N(1)	2.395(5)
O(1)−Ag(1)−N(3a)	108.4(1)	O(1)−Ag(1)−N(1)	90.7(2)
N(3a)−Ag(1)−N(3b)	116.0(2)	N(3a)−Ag(1)−N(1)	115.0(1)
Complex **4**[d]			
Ag(1)−N(1)	2.366(7)	Ag(1)−O(1)	2.490(7)
Ag(1)−N(2a)	2.384(7)	Ag(1)−N(3b)	2.404(7)
O(1)···O(3)	2.520(11)	O(2)···O(4)	2.752(13)
N(1)−Ag(1)−N(2a)	123.6(2)	N(1)−Ag(1)−N(3b)	115.9(2)
N(2a)−Ag(1)−N(3b)	108.4(2)	N(2a)−Ag(1)−O(1)	112.3(4)
N(1)−Ag(1)−O(1)	103.2(3)	N(3b)−Ag(1)−O(1)	87.1(3)
Complex **5**[e]			
Ag(1)−N(3a)	2.344(7)	Ag(1)−O(1)	2.449(7)
Ag(1)−N(1)	2.369(8)	Ag(1)−N(2b)	2.427(7)
O(1)···O(3)	2.518(10)	O(2)···O(4)	2.768(11)
N(3a)−Ag(1)−N(1)	125.0(2)	N(1)−Ag(1)−O(1)	110.5(4)
N(3a)−Ag(1)−N(2b)	117.6(2)	N(2b)−Ag(1)−O(1)	87.1(3)
N(1)−Ag(1)−N(2b)	106.9(3)	N(3a)−Ag(1)−O(1)	102.7(3)
Complex **6**[f]			
Ag(1)−N(2a)	2.374(5)	Ag(1)−N(1b)	2.384(5)
Ag(1)−N(3)	2.425(5)	Ag(1)−O(1)	2.583(6)
O(1)···O(4)	2.725(9)	O(1w)···O(4a)	3.004(9)
O(2)···O(1w)	2.868(10)		
N(2a)−Ag(1)−N(1b)	118.8(2)	N(2a)−Ag(1)−N(3)	107.4(2)
N(1b)−Ag(1)−N(3)	124.2(2)	N(1b)−Ag(1)−O(1)	85.8(2)
N(2a)−Ag(1)−O(1)	135.1(2)		
Complex **7**[g]			
Ag(1)−N(1)	2.380(5)	Ag(1)−N(3a)	2.427(5)
Ag(1)−N(2b)	2.427(5)	Ag(1)−O(1)	2.566(5)
N(4)···O(1w)	2.934(7)	O(1w)···O(2w)	2.942(9)
O(2w)···O(2c)	2.778(10)		
N(1)−Ag(1)−N(3a)	111.0(2)	N(1)−Ag(1)−N(2b)	114.6(2)
N(3a)−Ag(1)−N(2b)	123.4(2)	N(2b)−Ag(1)−O(1)	88.8(2)
N(1)−Ag(1)−O(1)	134.5(2)	N(3a)−Ag(1)−O(1)	82.2(2)
Complex **8**[h]			
Ag(1)−N(1)	2.351(4)	Ag(1)−N(2b)	2.439(3)
Ag(1)−N(2c)	2.439(3)	Ag(1)−O(1)	2.47(3)
Ag(1)−O(1d)	2.47(3)	N(3)···O(4w)	2.899(7)
O(2)···O(1w)	2.95(4)	O(1w)···O(2w)	2.772(12)
O(1w)···O(2e)	2.95(4)	O(2w)···O(3w)	2.852(11)
O(3w)···O(2a)	2.47(6)		
N(1)−Ag(1)−N(2b)	113.66(9)	N(1)−Ag(1)−O(1)	118.9(4)
N(2b)−Ag(1)−N(2c)	112.46(15)	N(2c)−Ag(1)−O(1)	104.5(6)
N(2b)−Ag(1)−O(1)	91.5(6)		

[a] Symmetry codes: a) x−1, y, z; b) x−1/2, −y−1/2, z+1/2; c) −x+1, −y, −z+1; d) −x+2, −y, −z+2; e) −x+3/2, y+1/2, −z+3/2. [b] Symmetry codes: a) x+1/2, −y+1/2, z+1/2; b) x+1, y, z; c) −x+1, −y+1, −z+2; d) −x+1/2, y+1/2, −z+3/2 [c] Symmetry codes: (a) $-x+1/2, -y, z-1/2$; (b) $-x+1/2, y+1/2, z-1/2$. [d] Symmetry codes: (a) $-x+1, -y, z-1/2$; (b) $x-1/2, -y, z$. [e] Symmetry codes: (a) $-x, -y+2, z-1/2$; (b) $-x+1/2, y, z-1/2$. [f] Symmetry codes: (a) $-x+3/2, y+1/2, z$; (b) $-x+1, y+1/2, -z+1/2$. [g] Symmetry codes: (a) $x, -y, z-1/2$; (b) $-x+1/2, y+1/2, z$; (c) $x+1/2, -y-1/2, -z+1$. [h] Symmetry codes: (a) $-x+1, -y+1, z$; (b) $x-1/2, -y+3/2, -z+3/2$; (c) $x-1/2, -y+3/2, z-1/2$; (d) $x, y, -z+1$; (e) $x, y, -z$.

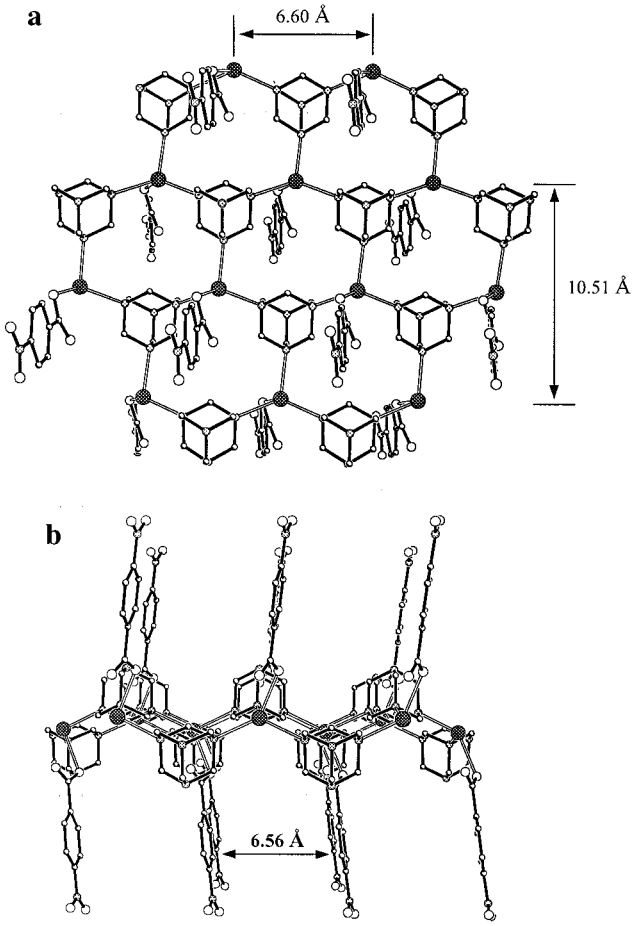

Figure 1. Top-view (a) and side-view (b) showing the [Ag(μ_3-hmt)] layer in **1**.

Results and Discussion

Synthesis Chemistry. Complexes **1**, **2**, and **3** were obtained by slow evaporation of MeCN−H_2O [2:1 (v/v)] solutions of Ag(μ_3-hmt)NO_3[5] and the corresponding benzoates in a molar ratio of 1:1; complexes **4**, **5**, and **6** were obtained by slow evaporation of CH_2Cl_2−EtOH−H_2O [10:10:1 (v/v)] solutions of Ag(μ_3-hmt)NO_3 and the corresponding aromatic carboxylates in a molar ratio of 1:1, while **7** and **8** were obtained from the reaction systems of hmt and the corresponding silver(I) dicarboxylates in MeCN−H_2O [2:1 (v/v)] solution in a molar ratio of 2:1. It should be mentioned here that the powder products for **7** and **8** obtained from the reaction systems of Ag(μ_3-hmt)-NO_3 and corresponding dicarboxylic acids in a MeCN−H_2O [2:1 (v/v)] solution in molar ratios of 2:1 have been proved to be identical with those of **7** and **8**, respectively, by elemental analyses and IR spectra.

All of these facts confirm that the 2-D hexagonal [Ag(μ_3-hmt)] networks are quite stable, and the methods for rational organization of the 2-D networks into 3-D networks via replacements of the small and labile anions with large aromatic monocarboxylates and linear dicarboxylate pillars are feasible.

Crystal Structures. The structure of **1** consists of 2-D infinite wavy neutral coordination layers of hexagonal units in a boat-type conformation, which are highly similar to those in [Ag(hmt)]X,[4−6,8b] as illustrated in Figure 1. Each hexagonal unit is organized by three Ag(I) ions and three hmt molecules each at the corner, in which the Ag(I) ion is in a distorted tetrahedral

(17) Sheldrick, G. M. *SHELXTL* Version 5; Siemens Industrial Automation Inc.: Madison, WI, 1995.

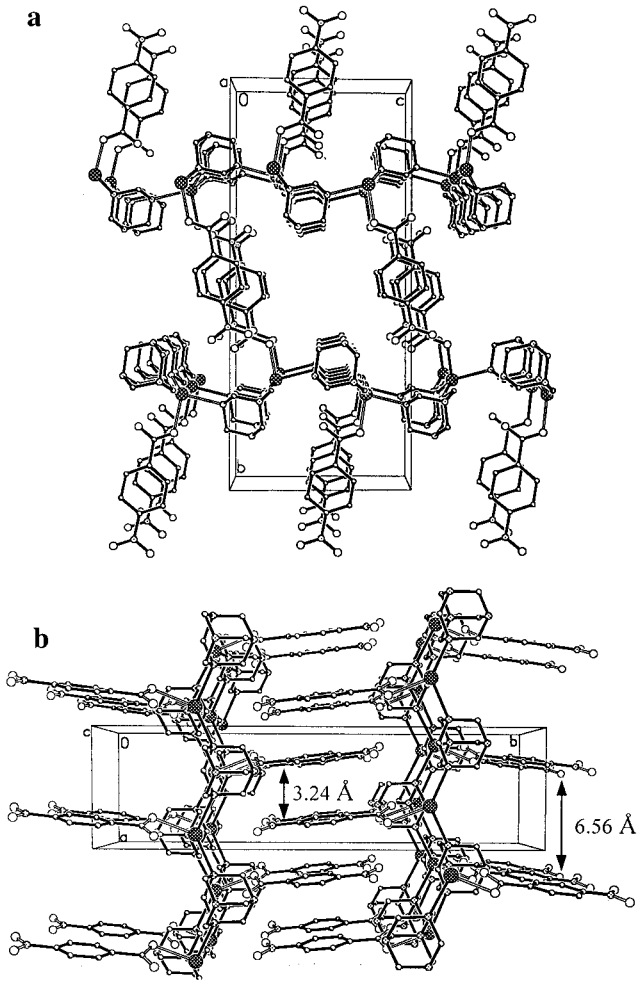

Figure 2. Perspective view showing the 3-D network along the *a*-axis (a) and *c*-axis (b) in **1**. The lattice water molecules are omitted for clarity.

geometry coordinated by three nitrogen atoms [Ag(1)−N = 2.378(3)−2.478(4) Å, N−Ag(1)−N 109.8(1)−117.0(1)°] from different hmt ligands and one monodentate *p*-nba ligand [Ag(1)−O = 2.367(4) Å, O−Ag(1)−N 87.3(1)−130.2(1)°]. Similar to the small anions in [Ag(hmt)]X (X = NO_3^- and NO_2^-), the *p*-nba ligands alternately orient vertically up and down in layers; the adjacent carboxylate groups within each row are separated at a distance of 6.60 Å, which resembles those (ca. 6.56 Å) found for the related [Ag(hmt)]X.[5,8b] These facts confirm our expectation that the 2-D hexagonal networks are suitable for organization of the 2-D networks into 3-D supramolecular architectures via intercalation of the lateral aromatic groups, since the gaps formed by the large aromatic groups in a parallel fashion are suitable for insertion of the aromatic groups from other layers. On the other hand, the row-to-row distance between the two rows with carboxylate groups oriented on the same side of the layer is 10.51 Å. As a result, adjacent layers are organized into a 3-D network by very strong $\pi-\pi$ stacking interactions of these aromatic rings from adjacent layers in an offset fashion with a face-to-face distance of 3.24 Å, resulting in a 3-D network having rhombic channels with an effective size of ca. 4 × 5 Å,[18] as shown in Figure 2. The free dimensions of these channels occupy 18.4% of the crystal volume.[19] The lattice water molecules are clathrated in these channels and form donor hydrogen bonds [O(2w)···O(1) 2.838(8); O(2w)···O(3) 3.028(8); O(3w)···N(3) 2.943(7) Å] with the coordinated carboxylate oxygen atoms, the nitro oxygen atoms, and the uncoordinated hmt nitrogen atoms.

The structures of **2** and **3** are very similar to that of **1**, featuring 2-D wavy layers of hexagonal units. The Ag(I) atom in **2** or **3** is also in a distorted tetrahedral geometry with the metal−ligand bond lengths and bond angles comparable to those in **1**, as listed in Table 2. The adjacent layers are, also similarly to that in **1**, organized into a 3-D network by similar intercalation featuring interlayer $\pi-\pi$ stacking interactions of these aromatic rings in an offset fashion with face-to-face distances of 3.21 Å in **2** and 3.26 Å in **3**. The free dimensions of these channels occupy 16.2% of the crystal volume in **2**, and the lattice water molecules are clathrated in these channels, forming donor hydrogen bonds similar to those in **1**. Due to the larger steric requirement of the two substituted nitro groups, the effective channels in **3** are much smaller than those in **1** and **2**; therefore, no guest solvent molecule is clathrated in these channels.

Similar to **1**−**3**, **4**−**6** also consist of 2-D infinite wavy neutral layers of hexagonal units, in which each unit is also organized by three Ag(I) ions and three hmt ligands each at the corner. The Ag(I) atom is in a greatly distorted tetrahedral geometry coordinated by three nitrogen atoms from different hmt ligands. The detailed geometric data are listed in Table 2. Although most of the geometric data are comparable to the corresponding values in **1**, it should be noted that in **4**−**6** the Ag−O bond lengths are much longer than those of Ag−N, in contrast to those in **1**−**3**. This fact shows that the Ag−O bonds in **4**−**6** are weaker than those in **1**−**3**, which may be responsible for the highly slanting orientation of the lateral aromatic ligands in **4**−**6**. Moreover, each pair of adjacent lateral aromatic groups in a row is orientated in two different directions. Therefore, the orientation is not suitable for intercalation of the aromatic groups from adjacent layers as that in **1**−**3**. Instead, the 2-D coordination layers in **4**−**6** are further extended via two ways, namely, weak $\pi-\pi$ stacking in a highly offset fashion and edge-to-face C−H···π stacking interactions, into 3-D supramolecular arrays different from those of **1**−**3**, as shown in Chart 2.

Viewed along the *a*-axis (Figure 3a), the aromatic carboxylates in **4** are alternately slanted up and down the hexagonal layer and the dihedral angles between the aromatic groups of the α-hna ligands and the 2-D layers are ca. 43°. Viewed along the *c*-axis (Figure 3b), the orientations of the adjacent aromatic rings at the same side of the coordination layer are alternately staggered, with a dihedral angle of 67°. The dihedral angles between the adjacent aromatic rings of adjacent layers are ca. 86°, resulting in a 3-D network with V-shaped channels running along the *a*-axis and triangular channels running along the *c*-axis. The free dimensions of these channels occupy 21.5% of the crystal volume. The ethanol molecules are clathrated in these channels and form donor hydrogen bonds [O(4)···O(2) 2.752(13) Å] with the uncoordinated carboxylate oxygen atoms.

The structure of **5** is quite similar to that of **4**, although the position of the hydroxy group is different. The minute difference is that the dihedral angles between the aromatic groups of the β-hna ligands and the 2-D layers are ca. 50°, and those between the adjacent aromatic rings of adjacent layers are ca. 82°. The free dimensions of the channels in **5** are equal to those in **4**, occupying 21.5% of the crystal volume. The ethanol molecules are clathrated in these channels and form donor hydrogen bonds [O(4)···O(2) 2.768(11) Å] with the uncoordinated carboxylate oxygen atoms.

(18) Hereafter the channel dimensions are estimated from the van der Waals radii for carbon (1.70 Å), nitrogen (1.55 Å), and oxygen (1.40 Å).

(19) Spek, A. L. *PLATON, A Multipurpose Crystallographic Tool*; Untrecht University: Utrecht, The Netherlands, 1999.

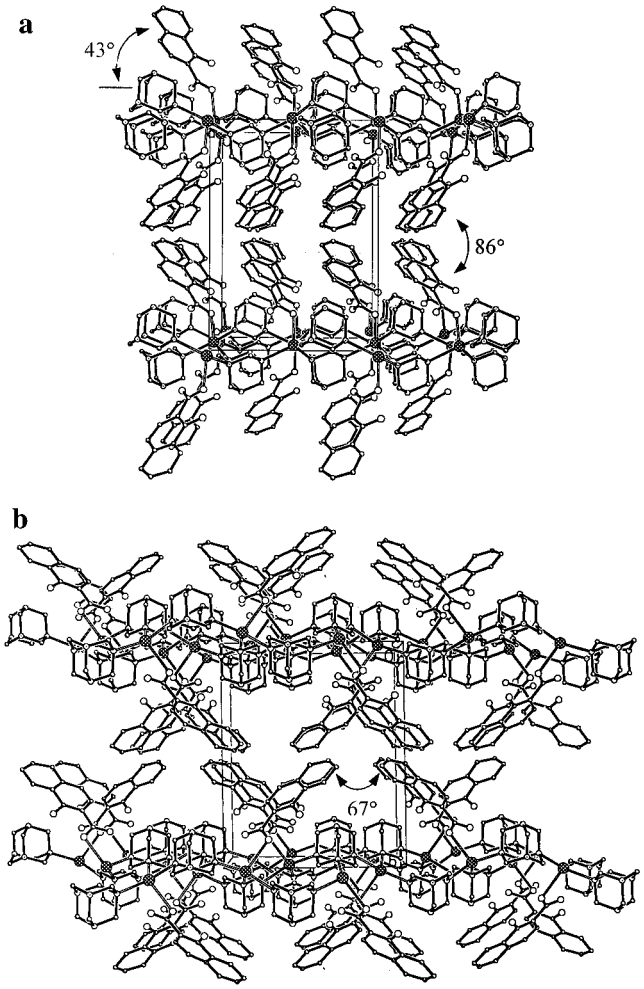

Figure 3. Perspective view showing the 3-D supramolecular arrays along the *a*-axis (a) and *c*-axis (b) in **4**. The lattice ethanol molecules are omitted for clarity.

The aromatic carboxylates in **6** are also alternately slanting up and down the hexagonal layer. Due to the presence of an ether group in noa, the aromatic rings in **6** are oriented in a different direction [C(2)−O(3)−C(3) 118.1(6)°], resulting in a dihedral angle of ca. 30° between the aromatic groups of the noa ligands and the 2-D Ag-hmt layers. Viewed along the *b*-axis, the orientations of the adjacent aromatic rings at the same side of the Ag-hmt layer are alternately staggered with a dihedral angle of 64°. Different from **4** and **5**, the adjacent aromatic rings of adjacent layers are almost parallel, resulting in a 3-D network with rhombic channels with an effective size of ca. 4 × 11 Å along the *a*-axis and triangular channels running along the *b*-axis, as shown in Figure 4. The free dimensions of these channels occupy 26.9% of the crystal volume. The lattice water molecules and ethanol molecules are clathrated in these channels and form donor hydrogen bonds [O(1w)···O(2) 2.868(10); O(4)···O(1) 2.725(9) Å] with the carboxylate oxygen atoms and the ether groups.

It is worthy of note that there are two different supramolecular interactions between the layers of **4**−**6**. In **4** and **5**, the edge-to-face separations of the adjacent aromatic rings between the adjacent layers are 3.63 Å (Figure 5a) and 3.72 Å, respectively, indicating significant C−H···π interaction,[20] while in **6**, the face-to-face distances of the adjacent aromatic rings between the adjacent layers in a highly offset fashion are 3.67 Å (Figure 5b), indicating significant interlayer $\pi-\pi$ stacking interaction.

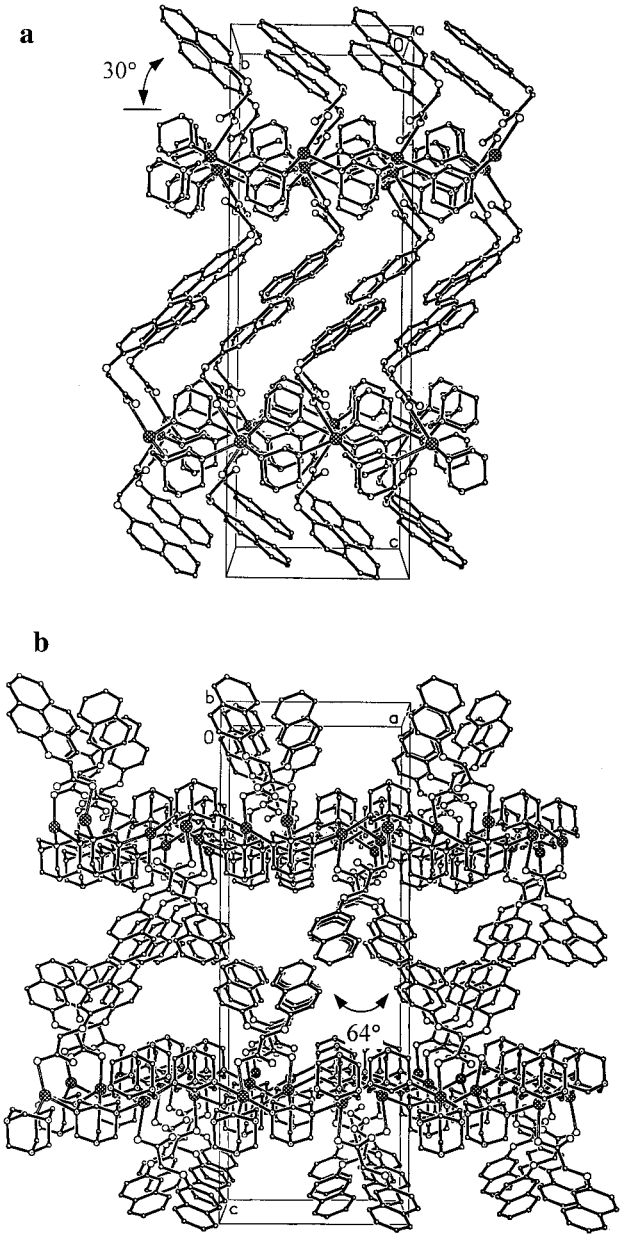

Figure 4. Perspective view showing the 3-D supramolecular arrays along the *a*-axis (a) and *b*-axis (b) in **6**. The lattice water and ethanol molecules are omitted for clarity.

Complexes **7** and **8** are two analogous microporous 3-D coordination networks constructed from 2-D Ag(μ_3-hmt) layers and linear dicarboxylates as molecular pillars.[21] In **7**, each Ag(I) ion is in a distorted tetrahedral geometry coordinated by three nitrogen atoms from different hmt ligands [Ag(1)−N 2.380(5)−2.427(7) Å, N−Ag(1)−N 110.96(5)−123.7(2)°] and one oxygen

(20) (a) Steiner, T.; Tamm, M.; Lutz, B.; Van der Mass, J. *J. Chem. Soc., Chem. Commun.* **1996**, 1127. (b) Madhavi, N. N. L.; Katz, A. K.; Carrell, H. L.; Nangia, A.; Desiraju, G. R. *J. Chem. Soc., Chem. Commun.* **1997**, 1953. (c) Weiss, H.-C.; Bläser, D.; Boese, R.; Doughan, B. M.; Haley, M. M. *J. Chem. Soc., Chem. Commun.* **1997**, 1703. (d) Biradha, K.; Seward, C.; Zaworotko, M. J. *Angew. Chem., Int. Ed.* **1999**, *38*, 492. (e) Tong, M.-L.; Zheng, S.-L.; Chen, X.-M. *Polyhedron* **2000**, *19*, 1809.

(21) (a) Michaelides, A.; Kiritsis, V.; Skoulika. S.; Aubry, A. *Angew. Chem., Int. Ed. Engl.* **1993**, *32*, 1495. (b) Shimizu, G. K. H.; Enright, G. D.; Ratcliffe, C. I.; Ripmeester, J. A. *Chem. Commun.* **1999**, 461. (c) Shimizu, G. K. H.; Enright, G. D.; Ratcliffe, C. I.; Ripmeester, J. A.; Wayner, D. D. M. *Angew. Chem., Int. Ed.* **1998**, *37*, 1407. (d) Hong, M.-C.; Su, W.; Cao; R.; Fujita, M.; Lu, J.-X. *Chem. Eur. J.* **2000**, *6*, 427

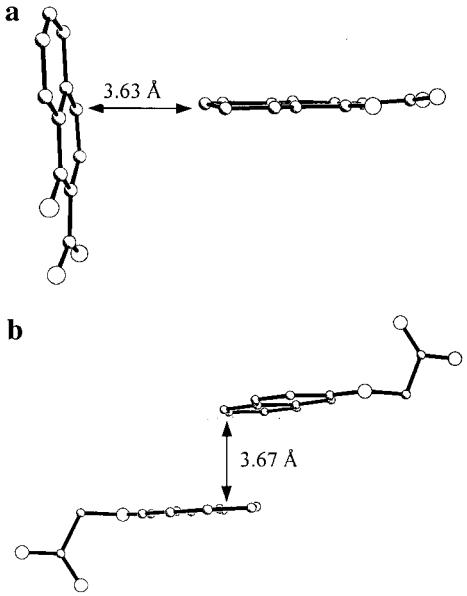

Figure 5. Perspective view showing the edge-to-face C−H···π interaction between the adjacent aromatic rings of the adjacent layers in **4** (a), and the offset face-to-face $\pi-\pi$ stacking interaction between the adjacent aromatic rings of the adjacent layers in **6** (b).

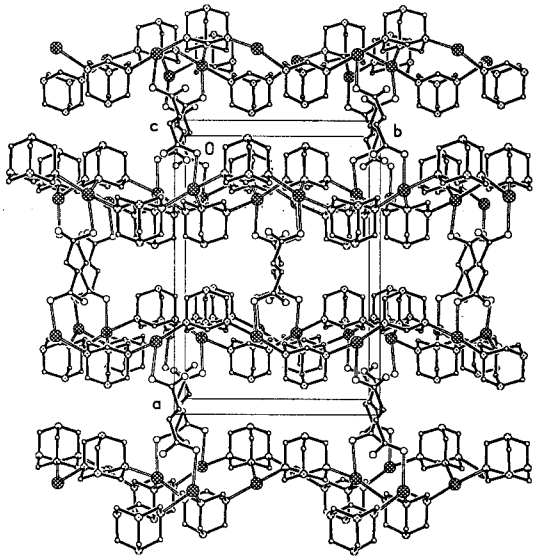

Figure 6. Perspective view showing the 3-D coordination network along the *c*-axis in **7**. The lattice ethanol molecules are omitted for clarity.

atom from a bis-monodentate fa ligand [Ag(1)−O 2.566(5) Å, N−Ag(1)−O 82.2(2)−88.8(2)°]. The dicarboxylate groups alternately orient up and down the 2-D hexagonal Ag-hmt layer, thus interconnecting the 2-D layers to generate a 3-D structure of channels with an effective size of ca. 2 × 8 Å running along the *c*-axis, as shown in Figure 6. The free dimensions of these channels occupy 12.5% of the crystal volume. The lattice water molecules are clathrated in these channels and form donor hydrogen bonds [O(2w)···O(2) 2.778(10); O(1w)···N(4) 2.934(7) Å] with the uncoordinated carboxylate oxygen atoms or the uncoordinated hmt nitrogen atoms.

Ag(I) atoms and hmt ligands in **8** are also interlinked into 2-D infinite wavy layers with hexagonal units, similar to that in **7**, and the adp groups also function in the bis-monodentate mode to pillar these layers into a highly similar 3-D structure without interpenetration. This network yields channels with an effective size of ca. 3 × 10 Å along the *a*-axis and ca. 4 × 5

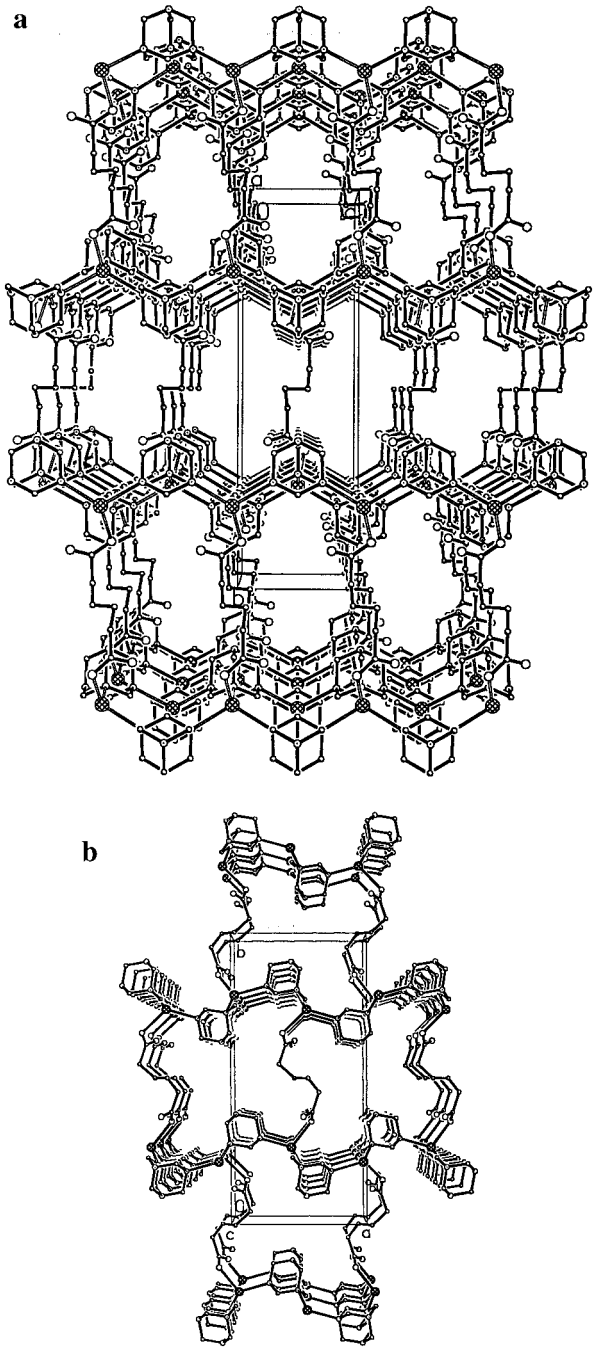

Figure 7. Perspective view showing the 3-D coordination network along the *a*-axis (a) and *c*-axis (b) in **8**. The lattice ethanol molecules are omitted for clarity.

Å along the *c*-axis, as shown in Figure 7, significantly larger than that in **7**. The free dimensions of these channels occupy 20.9% of the crystal volume.

Thermogravimetric Analysis. To examine the thermal stability of the porous networks, thermal gravimetric (TG) analyses were carried out. The TGA curve for **1** shows that the first weight loss of 9.6% between 70 and 120 °C corresponds to the loss of the lattice water molecules (calcd 9.8%). Decomposition of **1** began above 208 °C. The TGA curve for **2** shows that the first weight loss of 8.8% between 70 and 120 °C corresponds to the loss of two lattice water molecules (calcd 9.8%). Decomposition of **3** began above 200 °C. The TGA curve for **4** shows that the first weight loss of 9.5% between 76 and 110 °C corresponds to the loss of the solvate ethanol molecules

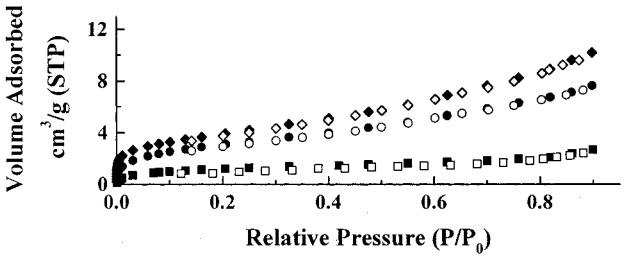

Figure 8. Gas adsorption isotherms for the anhydrous **1**, **6**, and **8** [the adsorption of the desolvate **1** (■), **6** (●), and **8** (◆); the desorption of the desolvate **1** (□), **6** (○), and **8** (◇)].

(calcd 9.6%). Decomposition of **4** began above 205 °C. The TGA curve for **5** shows that the first weight loss of 12.1% between 75 and 126 °C corresponds to the loss of the lattice water molecules and ethanol molecules (calcd 12.5%). Decomposition of **5** began above 174 °C. The TGA curve for **6** shows that the first weight loss of 11.9% between 76 and 124 °C corresponds to the loss of the lattice water molecules and ethanol molecules (calcd 12.5%). Decomposition of **6** began above 175 °C. The TGA curve for **7** shows that the first weight loss of 10.2% between 70 and 120 °C corresponds to the loss of the lattice water molecules (calcd 10.6%). Decomposition of **7** began above 200 °C. The TGA curve for **8** shows that the first weight loss of 19.0% between 50 and 92 °C corresponds to the loss of one lattice water molecule (calcd 18.4%). Decomposition of **8** began above 203 °C.

The above observations show that the microporous compounds reported in this paper are stable up to ca. 200 °C, suggesting that they may, in a sense, be related to the porous materials.

Gas Adsorption Isotherm. In view of the microporosity of the Ag-hmt frameworks, we selected three compounds with larger channels**, 1**, **6**, and **8**, for the gas adsorption measurements. As shown as Figure 8, the gas adsorption isotherms for desolvate **1**, **6**, and **8** were at low levels (1.08, 1.41, and 3.31 mL/g, respectively) with $0.1P_0$ (P_0 = saturation pressure), while at much higher levels (2.01, 7.68, and 10.2 mL/g, respectively) with $0.9P_0$. The pore size distributions of desolvate **1**, **6**, and **8** were calculated, and the data were fitted to a Horvath−Kawazore differential pore volume (HK) plot.[22] The HK plot showed one peak at about 7.8, 11.6, and 9.6 Å for the desolvate **1**, **6**, and **8**, respectively, which agrees with the results of X-ray analysis, and the deviations compared with the crystal structural results should be ascribed to the irregular shapes of the channels.[3e]

Conclusions

The interesting microporous networks, based on 2-D Ag(I)-hmt coordination layers, have been obtained by design and synthesis. The isolations and characterizations of these eight complexes demonstrate the possibility of designed assembly of the hexagonal 2-D Ag-hmt layers into 3-D microporous networks via replacements of the small and labile lateral anions with large aromatic monocarboxylates or dicarboxylates, suggesting new strategies for construction of microporous coordination materials with tuneable channels.

Acknowledgment. This work was supported by the National Natural Science Foundation of China (No. 29971033 & 29625102). We are indebted to the Chemistry Department of The Chinese University of Hong Kong for donation of the diffractometer.

Supporting Information Available: Eight X-ray crystallographic files, in CIF format, for the structure determination of **1**−**8**. This material is available free of charge via the Internet at http://pubs.acs.org.

IC001237Z

(22) Horvath, G.; Kawazoe, K. *J. Chem. Eng. Jpn.* **1983**, *16*, 460